*IOSR Journal Of Applied Physics (IOSR-JAP)*
*e-ISSN: 2278-4861.Volume 12, Issue 2 Ser. I (Mar. – Apr. 2020), PP 10-19*
*www.Iosrjournals.Org*

# Synthesis of Zinc Oxide Nanoparticles via Sol-gel Technique

Umme Habiba[1], M.N.H. Mia[2], Afroza Khatun[1], Rezvi Ahamed Ratul[1], DewanShabbir Ahmed[1], Shakhawat Hossain[1],Mijanur Rahman[1], Humayun Kabir[3*]

[1]*Department of Physics, MawlanaBhashani Science and Technology University, Santosh, Tangail-1902, Bangladesh.*
[2]*Institute of Electronics, Atomic Energy Research Establishment, Bangladesh Atomic Energy Commission, Dhaka 1349, Bangladesh.*
[3]*Department of Physics, Jahangirnagar University, Savar, Dhaka-1342, Bangladesh.*

[*]*Corresponding Author's Email:rumy140@juniv.edu*

***Abstract:*** *In this work, Zinc Oxide nanoparticles (ZnO-NPs) were successfully synthesizedvia a facile sol-gel techniqueusingzinc acetate dehydrate, triethanolamine, ethanol and ammonium hydroxide. Characteristics of the as synthesizedZnO-NPs were studied via X-Ray diffraction (XRD), environmental scanning electron microscopy (ESEM), energy-dispersive X-ray spectroscopy, Fourier transform infrared spectroscopy, thermo gravimetric analysis,ultraviolet visible (UV-Vis) spectroscopy and photoluminescence spectroscopy. The XRD patterns confirmed the hexagonalwurtzite structure of ZnOwith lattice constant values, a = b = 3.2488 Å and c = 5.2054 Å. The average size of NPs estimated from ESEM images were in good agreement with the average crystal size obtained from the XRD data.The average particle size estimated from ESEM micrographs for sol-gel synthesis of ZnO-NPs was nearly 60 nm. The EDS study confirmed the presence of Oxygen and Zinc in the ZnO-NPs. The computed value of optical band gap was found to be 3.18 eV. The photoluminescencespectra revealed a strong emission band located at a wavelength of375 nm which is a typical UV band. This may be ascribed to the exciton recombination related near-band edge emission ofZnO. A week blueband at 465 nm was also observed which is owing to the electron transition from the conduction band to interstitialoxygen defects ($O_{in}$) in the ZnO.*

***Key Words****: Sol-gel method, X-Ray diffraction, particle size, lattice strain, lattice constant.*

---

Date of Submission: 29-02-2020 Date of Acceptance: 14-03-2020

---

## I. Introduction

Nanomaterial is composed of particles having nano-scale dimension called nanoparticles (NPs).They are very small sized particles (particle sizes in the range 1-100 nm) exhibiting enhanced catalytic reactivity, thermal conductivity, non-linear optical performance and chemical steadiness owing to its large surface area to volume ratio [1, 2]. NPs have found wide applications in nano-engineering and nanotechnology, and is a fast developing area of research in science and technology. This is because NPs have unique properties, which are not present in bulk materials and can be exploited in numerous areas of science, industry and medicine. NPs have started being considered as nano-antibiotics because of their antimicrobial activities [3, 4]. NPs have been integrated into various industrial, health, food, feed, space, chemical, and cosmetics industry of consumers which calls for a green and environment-friendly approach to their synthesis [5-7]. A number of inorganic metal oxides, such as CeO, $L_2O_3$, $TiO_2$, CuO, and ZnO [8, 9, 10, 11] were synthesized using different techniques including sol-gel, hydrothermal, solvo-thermal, microwave, etc. [12]. Of all these metal oxides, ZnO NPs is of highest interest because they are inexpensive to produce, safe and can be prepared easily [12, 13]. Moreover, they possess several novel properties, such as large band gap (3.37eV) and high exciton binding energy (60 meV), high refractive index, binding energy, large thermal conductivity, high catalytic activity, antibacterial, UV filtering properties, anti-inflammatory, wound healing [14-19]. ZnO has also high biocompatibility and fast electric transfer kinetics, such phenomena encourage the use of this material as a biomimic membrane to immobilize and modify the biomolecules [20]. In many literatures, it is found that nano ZnO offers better performance compared to that of bulk size ZnO [21]. Zinc is a necessary element to our health and ZnO nano particles also have good biocompatibility to human cells [22, 23]. Recently ZnO is listed as generally documented as safe material by FDA (food and drug administration, (US A) [23].A numerous techniques have been used to prepare ZnO nanoparticles including sol-gel method, hydrothermal, microwave, solvothermal, thermal decomposition, chemical vapor decomposition (CVD) and alloy evaporation-deposition, laser

deposition [24-30]. A simple, fast wet chemical route based on cyclohexyl amine for synthesizing zinc oxide nanoparticles in aqueous and ethanolic media was established by Abdul-AzizBari [31], and observed that when NH4OH is used as the solvent for zinc acetate to synthesis nano ZnO particles, the particles were spherical, while the particles were wire like when sodium hydroxide was used as solvent. Also, the results of Zaborski [32] revealed the morphology of ZnO which was prepared in the presence of the ionic liquids was spherical while it changed to plate-like without ionic liquids. It is demonstrated that ZnO with different morphologies such as flowers and rods can be controllable obtained by simply varying the basicity in the solution [32]**.**

In brief, the solvents, temperature and media of experiment affect the particle size and particle morphology of synthesized ZnO nanoparticles. The aim of this research is to find a simple route to prepare nano ZnO particles via Sol-Gel technique and characterize the final product using several characterization techniques including X-ray diffraction (XRD), Energy-dispersive X-ray spectroscopy (EDX), scanning electron microscopy and ultraviolet-visible (UV-Vis) spectroscopy.

## II. Experimental Details

### *2.1 Raw materials used for the synthesis of ZnO NPs*

All chemicals including Zinc acetate dehydrate (purity 99%), triethanolamine (purity 99%), Ethanol and ammonium hydroxide were analytical reagent grade, and were purchased from Sigma Aldrich, UK. They wereused withoutany further purification.

### *2.2 Sol-Gel synthesis process ZnO NPs*

First of all, in a 100ml beaker 30 ml of water was added with 35 ml of triethanolamine(TEA) and drop wise ethanol was added with continuous stirring to get a homogeneous solution. After addition of 100 drops ethanol that was about 3 ml and continuous stirring results a homogeneous solution. Keeping the stoichiometry in mind a 2.0 gm batch of zinc oxide was prepared. Firstly, 30ml of water was mixed with 20 ml of TEA with constant stirring and drop wise addition of ethanol. Theobtained homogeneous solution was kept at rest for 3.0 hours. Simultaneously, as per the molar calculation for 2.0 gm batch of zinc oxide 5.49gm of zinc acetate di-hydrate was mixed with 50ml water and 0.5M of solution was prepared which was subjected to continuous stirring to get a homogeneous solution. After that the two solutions were mixed together in 500ml beaker and drop wise ammonium hydroxide was added with continuous heating and stirring for 20minutes*via* hot plate. Nearly 10ml of distil water was added during stirring. Then the solution was left for half an hour which results in the formation of white bulky solution. The obtained solution was then washed 10-12 times with distil water and filtered in a filter paper. The residue obtained waskept for drying in an oven at a temperature of about 95°C for 6 hours. The yellowish white powder obtained was then subjected to calcinations at a temperature of600°C for 5 hours.

### *2.3 Characterization ofZnO NPs*

The structural characterization was performed using an Equinox 3000 X-ray powder diffractometer in the 2θ range from $10^o$ to $60^o$, and step of $0.03^0$, with graphite monochromatic Cu Kα radiation(λ = 0.154 18 nm) at operating voltage of 35 kV and current of 25 mA.The surface morphology and particle size of ZnONPs were measured by using a Philips XL 30 ESEM equipped with Oxford INCA EDX FEG electron microscope operated at 20 kV at different magnifications. The analysis was performed on the SEM mode under high vacuum condition.To prepare a sample for ESEM, 1.0 mg of ZnO NPswas suspended in 5.0 ml of ethanol and bath-sonicated for 20 minutes by using an ultra-sonication bath (FB15046, Fisherbrand). A drop of the resulting solution was placed onto a thin Cu coating film which was set previously on a steel stab.The EDS of the samples was performed by a Philips XL 30 ESEM and EDX FEG electron microscope operated at 10 kV at different magnifications.The FTIR spectra were recorded in transmittance (%) mode at room temperature by using a double beam IR spectrophotometer (Nicolet 8600 FTIR spectrometer) in the wavenumber range from 400 to 4000 $cm^{-1}$. To obtain the IR spectra, a ratio of 1:100 of the sample and potassium bromide, KBr were used. The background using a control sample of KBr was always taken prior to each measurement. The applied resolution and number of scan was 4 $cm^{-1}$ and 100 per minute, respectively. TG and DSC analysis of the as synthesized ZnO NPs were carried out from room temperature 25 $^0$C to 1000 $^0$C at a heating rate of 10 $^0$C /min under argon gas flow by a NETZSCH Thermal Analysis STA 449C with pairs of matched platinum-rhodium crucibles. The opticalproperties of the as synthesized ZnO NPs were determined by UV-Vis spectrometer (Shimadzu model UV−3600) in the reflectance mode at room temperature in the range of 200-700 nm.The PL spectra were recorded by a QuantaMaster $^{TM}$ 510 spectrofluoro-meter (HORIBA Jobin, Germany) equipped with a xenon lamp light source for excitation (with excitation wavelength, $\lambda_{ex}$ = 300 nm) at room temperature.

## III. Results and discussion

### 3.1. XRD analysis

#### *3.1.1. Phase Identification and Lattice constant determination*

X-ray diffraction patterns for as synthesizedZnO NPsis shown in Fig.1. An X-ray pattern presented in Fig.1 reveals the overall crystal structure and phase purity of the synthesizedZnO NPs. All of the diffraction peaks of the ZnO NPs were indexed to (100), (002), (101), (102), (110), (103), (200), (112), (201), (004) and (202) planes in close correlation with lattice planes of hexagonal wurtzite structure of ZnO.The strong and sharp diffraction peaks with prominent intensity reflect the high crystallinity in ZnONPs and the detectable peaks matches well with the JCPDS card No. 36-1451. All of the characteristic peaks of ZnO lie in the range of $20°<2\theta<80°$ it further confirms the form of metal oxide (ZnO). As there is no additional peak in the XRD patterns, it indicates the high purity of the as synthesizedZnO NPs. From the *d*-spacing values,the lattice constants, *a* and *c* of the unit cell for hexagonal structure of ZnO, were calculated by the following equation[33],

$$\frac{1}{d_{hkl}^2} = \frac{4}{3}\left(\frac{h^2 + hk + k^2}{a^2}\right) + \frac{l^2}{c^2} \qquad (1)$$

where$d_{hkl}$ is the interplanar spacing of the atomic planes and hkl is Miller indices.The value of lattice parameters *a*, *b* and *c* of the ZnO NPs were calculated using Equation (1)and was found to be 3.2488, 3.2488, and 5.2054 Å and these values were alsoin good agreement with the values reported inliterature.

#### *3.1.2. Crystallite size and strain*

In the X-ray diffraction pattern, the broadening of peaks appears owing to both instrumental as well as sample factors. That is way, it is necessary to correct first the broadening due to instrument. The remaining broadening is then ascribed to sample related factors which include broadening because of the crystallite size and strain. The corrected broadening of the diffraction peak ($\beta_C$) can be determined by the following relation:

$$\beta_C^2 = \beta_M^2 - \beta_I^2 \qquad (2)$$

where$\beta_M$ and $\beta_I$ are the measured broadening due to sample and that of the instrument, respectively.

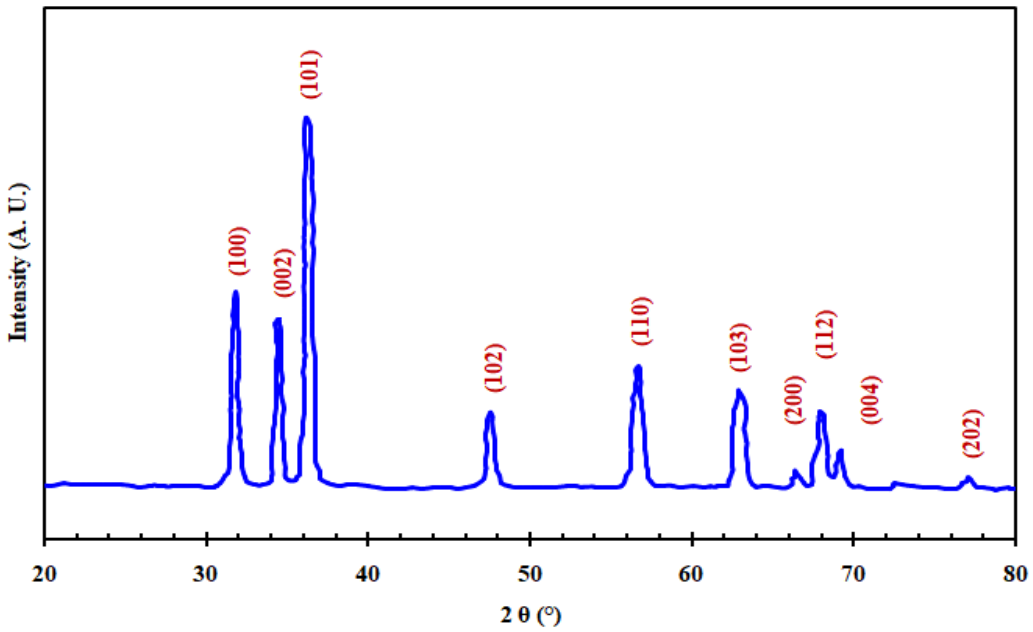


**Figure1:** XRD patterns of ZnO NPs.

The width of the diffraction peak varies with the crystallite or grain size of the sample. Diffraction peak broadening occur for very tiny crystals or grain. The crystallite size of the measured sample can be found by using the Scherrer's formula [7],

$$D = \frac{K\lambda}{\beta cos\theta_B} \qquad (3)$$

where *D* is the diameter of the crystallite, $\beta$ is the full width at half maximum (FWHM) of the selected diffraction peak, $\theta_B$is the Bragg angle, $\lambda$ is the wavelength of the X-ray used, and *K* is a constant of which the value depends on the shape of the crystallite. The value of K is equal to 0.9 for spherically shaped crystals. The calculated value ofcrystallite size was 28 nm.

The FWHM of the XRD peaks may also contain contributions from lattice strain, $\varepsilon_{str}$ and the strain induced in powders owing to crystal imperfection and distortion can be calculated by using the Stokes-Wilson equation [34],

$$\varepsilon_{str} = \frac{\beta_C}{4\ tan\theta} \qquad (4)$$

The calculated value oflattice strain determined by using Equations (4)was0.0041.

### *3.1.3. Dislocation density and Unit cell volume*

A variety of properties ofthe materials is strongly affected by crystallographic defects or irregularity within a crystal structure. This defects or irregularity is known as dislocation. In crystalline solids, atoms or molecules exist in a periodic nature and repeat fixed distancepositions which can be found by a parameter called the unit cell parameter.This regular pattern in a crystal is interrupted by dislocations. The dislocation density, $\delta$ for ZnO NPscan be determined by the expression [35]:

$$\delta = \frac{15\beta cos\theta}{4aD} \qquad (5)$$

where symbols have their usual meanings.The unit cell volume, *V* for hexagonal ZnO NPs wascalculated by using the following relation [36]:

$$V = \frac{\sqrt{3}}{2} a^2 c \qquad (6)$$

where*a* and *c* are the lattice constants for ZnO NPs.The calculated value of $\delta$and *V* for as synthesized ZnO NPs is 0.0005 and 47.5793$Å^3$, respectively.

### *3.1.4. Crystal index*

The crystalinity of the as synthesized ZnO NPs can be represented by the crystal index, $C_i$ and can be calculated with the help of XRD data by the following expression [37]:

$$C_i = \frac{I_{max}}{\beta_c} \qquad (7)$$

In this case $I_{max}$is the maximum intensity of the XRD peak and $\beta_c$ is the value of corrected FWHM.The computed value of $C_i$and c/a ratio for as synthesized ZnO NPs is 5622.58 and 1.6023, respectively.

## 3.2 Surface Morphology and Particle Size Measurement

The grain size, shape and surface properties, such as the surface morphology of the synthesizedZnO NPs were illustrated with the help of ESEM micrographs at different magnifications. Figs.2 and 3 represent the SEM micrographs of the as synthesized ZnO NPs samples at different magnifications. It is found from Figs.2 and 3 that the sol-gel synthesis of ZnO NPs is mostly ball like uniform shaped particles and capsules shape nanoparticles with very fine agglomeration. The particle size at different magnification for as synthesized ZnO NPs samples is 60 nm which is very good agreement with the results obtained from the XRD study[20, 29].

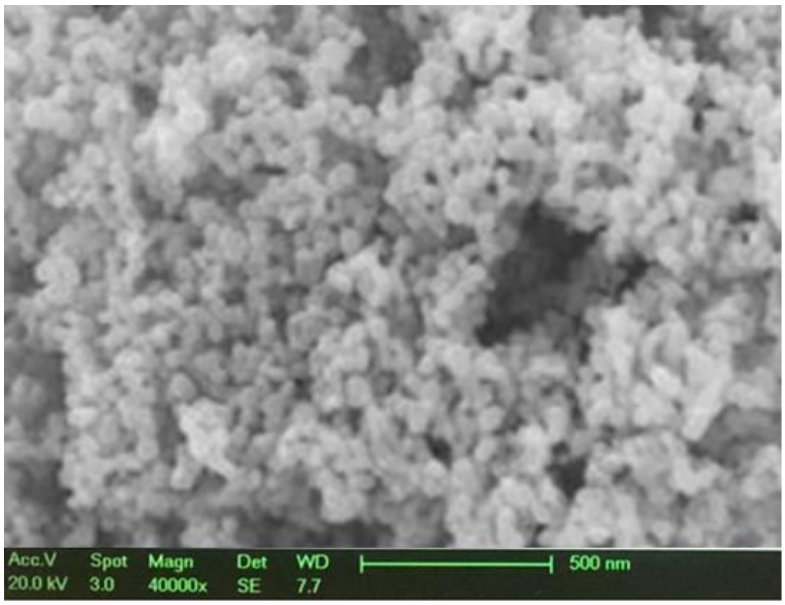


**Fig. 2:** SEM micrographs of ZnO NPs sample at magnification 40k×.

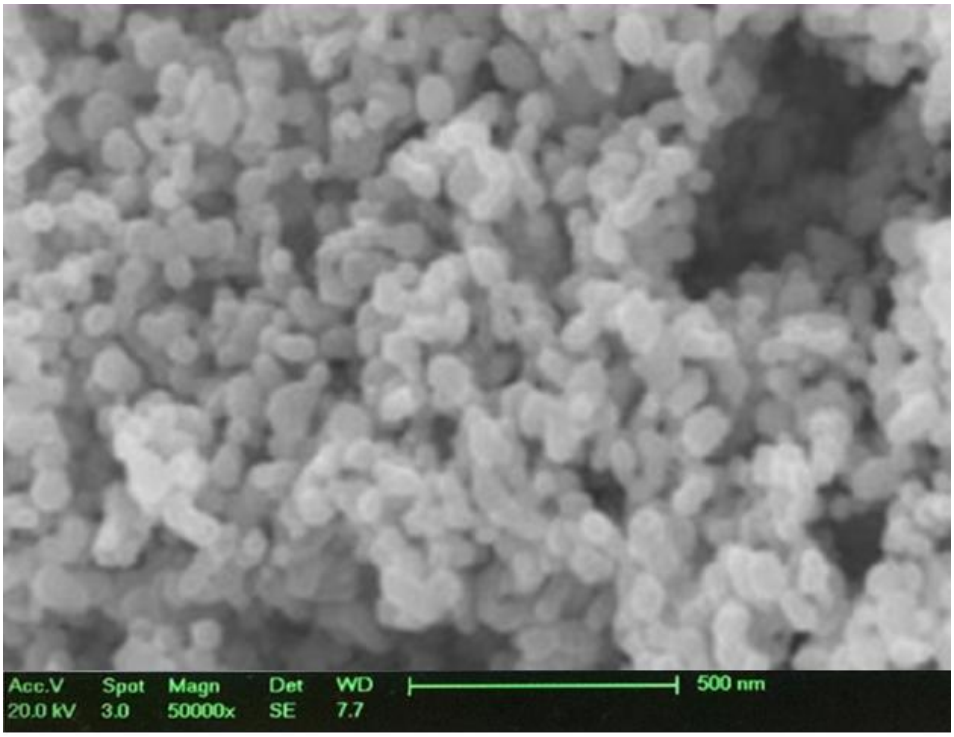


**Fig. 3:** SEM micrographs of ZnO NPs sample at magnification 50k×.

### 3.3 Chemical Composition Study

The EDS spectra of ZnO NPs samples calcined at a temperature 600 °Care represented in Fig.4. The weight percentage (wt. %) of the Zinc (Zn), Oxygen (O) and Carbon (C) are 87.69, 8.98, and 3.33%, respectively. The results confirmed the presence of Oxygen (O) as well as Zinc (Zn) in agreement with previous work. Some carbon was also present most likely due to the carbon adhesive tape used to secure the samples on the SEM stabs.

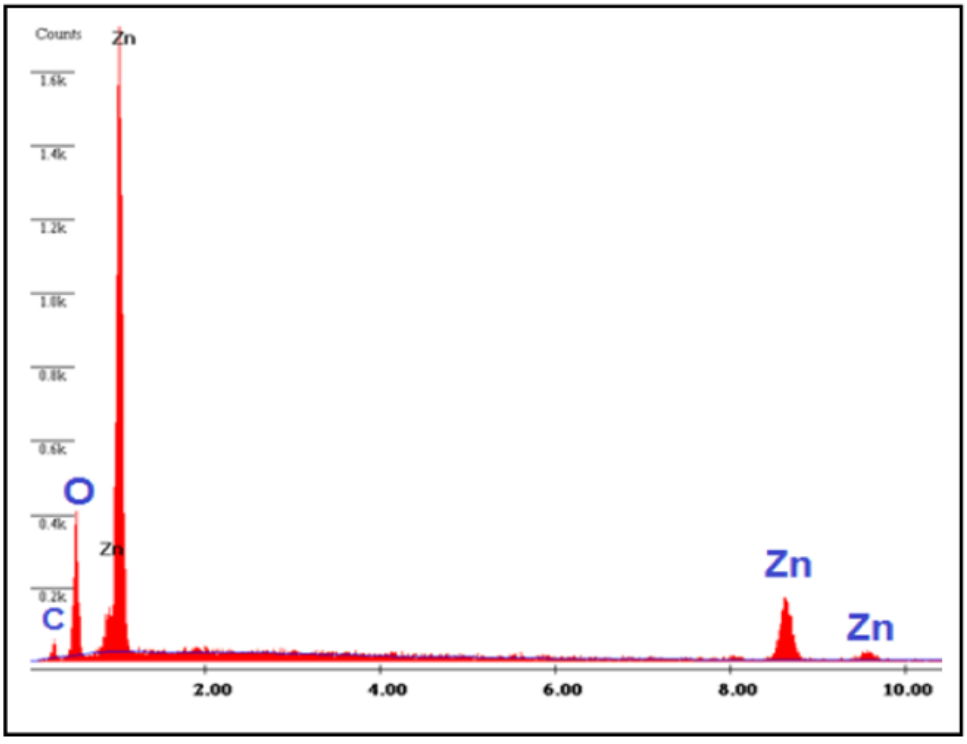


**Fig. 4:**EDS spectra of ZnO NPs sample.

### 3.4 Fourier Transform Infrared Spectroscopy analysis

The FTIR spectrum of the as synthesized ZnO NPs in the wavenumber range 4000-400 $cm^{-1}$ isillustrated in Fig.5. In the spectrum of the sampleshown in Fig.5, a broad band is observed at the wavenumber of 3507 $cm^{-1}$and this band shows the presence of O-H stretching vibration which is due to absorbed moisture on the surface of the samples. The absorption peaks at 1635$cm^{-1}$ is because of H-O-H bending vibrations.The peaks at 2390 $cm^{-1}$are attributed to the presence of carbon dioxide. Theabsorption picks around 1392 $cm^{-1}$ is assigned to thebending vibration of C-H stretching. The peaks at 514 to442 $cm^{-1}$ are for Zn-O[38]. The above results are inaccordance with the XRD results.

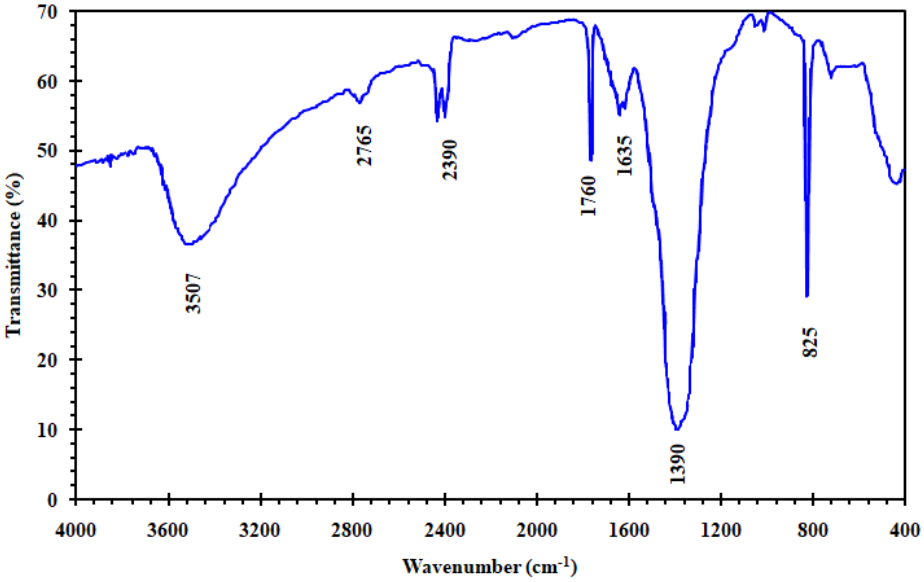


**Fig. 5:**FTIR spectrum of ZnO NPs samples.

### 3.5 Thermal analysis of ZnO NPs

TGA trace of the as synthesized ZnO NPs were used in the temperature range 30-1000 $^0$C at a scan rate of 10 $^0$C /min in argon atmosphere to investigate deeply the thermal decomposition of the samples. Fig. 6 representsthe TGA curve of the as synthesized ZnO NPs. It is observed from Fig. 6 that a small amount of weight loss has occurred around 100°C, thereby indicating theevaporation of water and/or moisture. As the DSC & TGA was carried out after calcination of the sample, so the DSC curve obtained shows multistate decomposition without forming any intermediates.

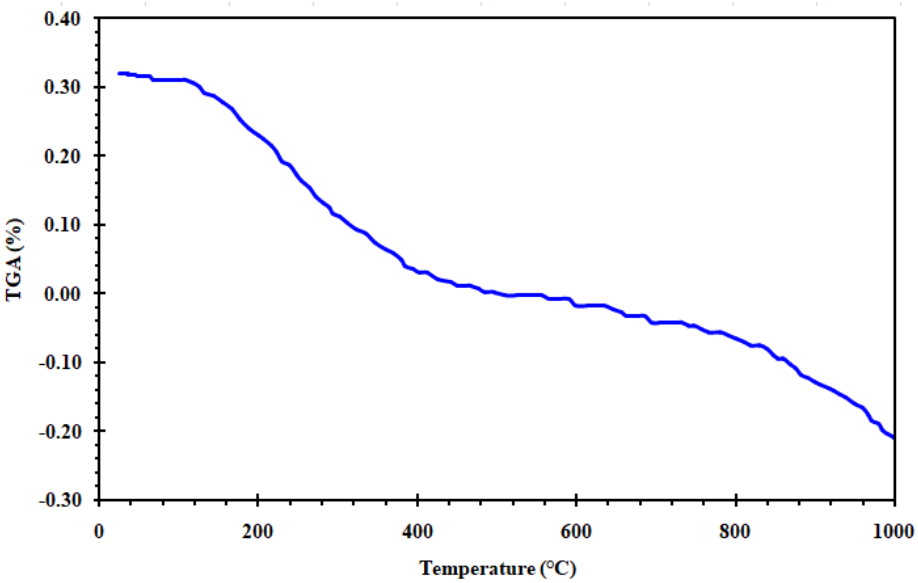


**Fig. 6:**TGA trace of the as synthesized ZnO NPscalcined at a temperature of 600 °C.

### 3.6 Ultraviolet visible Spectroscopy Study

The UV-Vis spectrum in reflectance mode was carried out to study the optical proper ties of the as synthesized ZnO NPs and is shown in Fig.7. It is seen from Fig.7 that the diffused reflectance spectra showed asharp increase at 380 nm and the material had a strong reflective characteristic after approximately 450 nm. This was due to the high possibility ofreflectance for the photons lacking the required energy forinteracting with electrons or atoms. It was observed that theabsorption of the ZnO nanoparticles was strongly affected bythe particle sizes. The band gap energies were determined using Kubelka-Munk function[39]:

$$F(R) = \frac{\alpha}{S} = \frac{(1-R)^2}{2R} \qquad (8)$$

Where $\alpha$ is given as the absorption coefficient, $S$ is denoted as the scattering coefficient, ($R$) is the absolute value of reflectance and $F(R)$ is known as the Kubelka-Munk function. For the diffused reflectance spectra, the Kubelka-Munk function could be used instead of absorption coefficient $\alpha$ for the evaluation of the optical absorption edge energy. The plot of $[F(R)\cdot h\nu]^2$against $h\nu$ (eV) was linear near the edge for direct allowed transition ($n$= 1/2). Here$h\nu$is the photon energy. The intercept of the line on the abscissa $[F(R)\cdot h\nu]^2$= zero) gives the optical band gap energy of the samples [40, 41]. The Fig.8 shows the variation of $[F(R)\cdot h\nu]^2$versus $h\nu$ plot for as synthesized ZnO NPs. The estimated value of optical band gap for our as synthesized ZnO NPs is 3.18 eV.

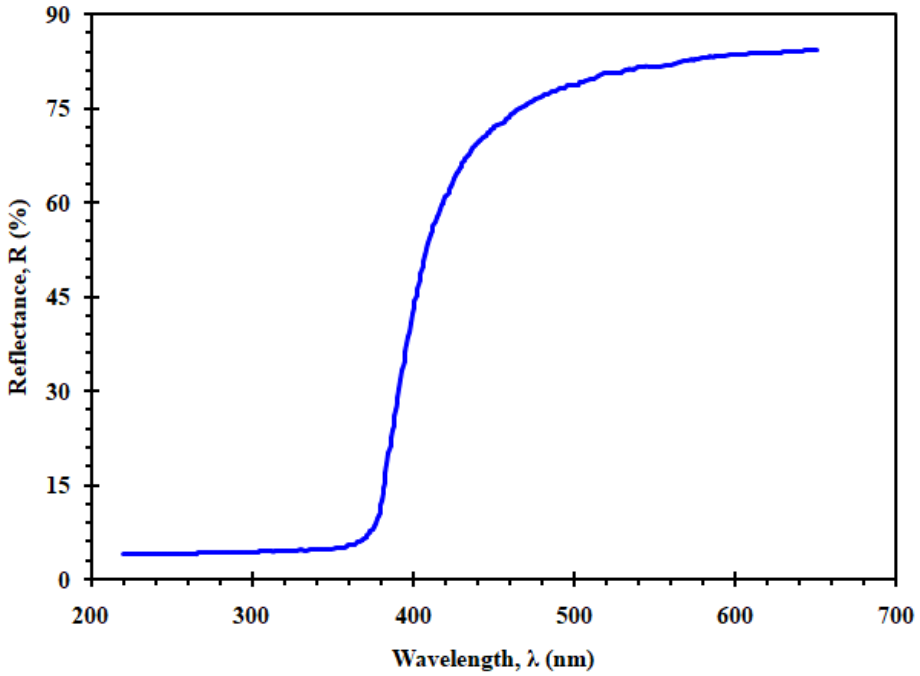


**Fig.7:**Diffuse reflectance spectra of the ZnO nanoparticles.

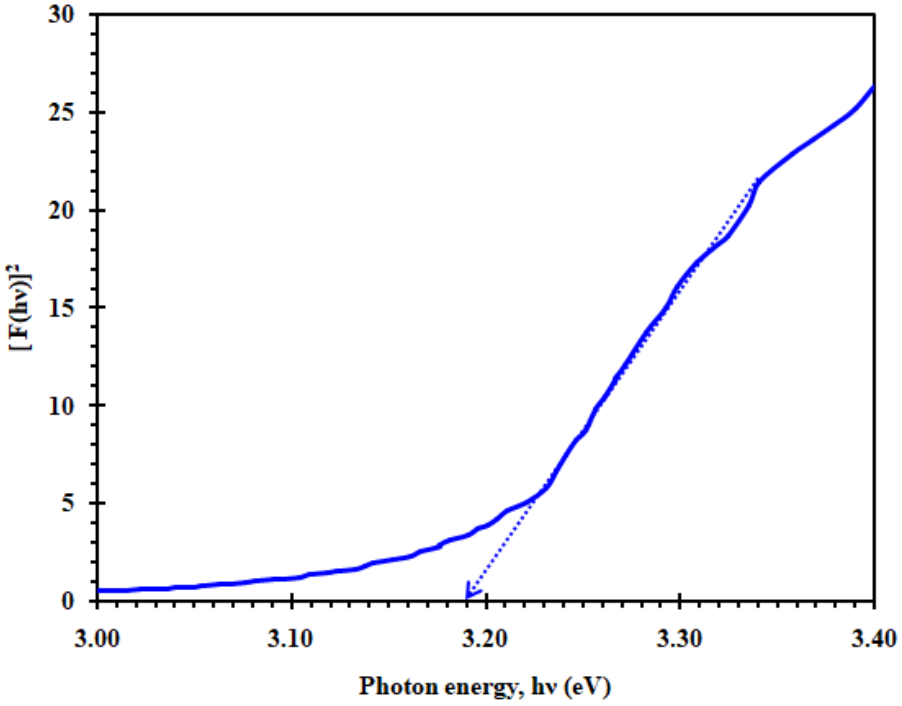


**Fig. 8:**Band gap energy of sol-gel synthesize ZnO nanoparticles.

### 3.7 Photoluminescence Spectroscopy Study

The Photoluminescence (PL) spectrum of the sol-gel synthesis of ZnO NPs is illustrated in Fig.9. From Fig.9 it is seen that the strongest emission band is found to be located at the wavelength of 375 nm. The observed emission band at 375 nm is a typical UV band. This may be ascribed to the exciton recombination related near-band edge (NBE) emission ofZnO. A week blueband at 465 nm was also observed which is due to the electron transition from the conduction band to interstitialoxygen defects ($O_{in}$) in the ZnO[42, 43].

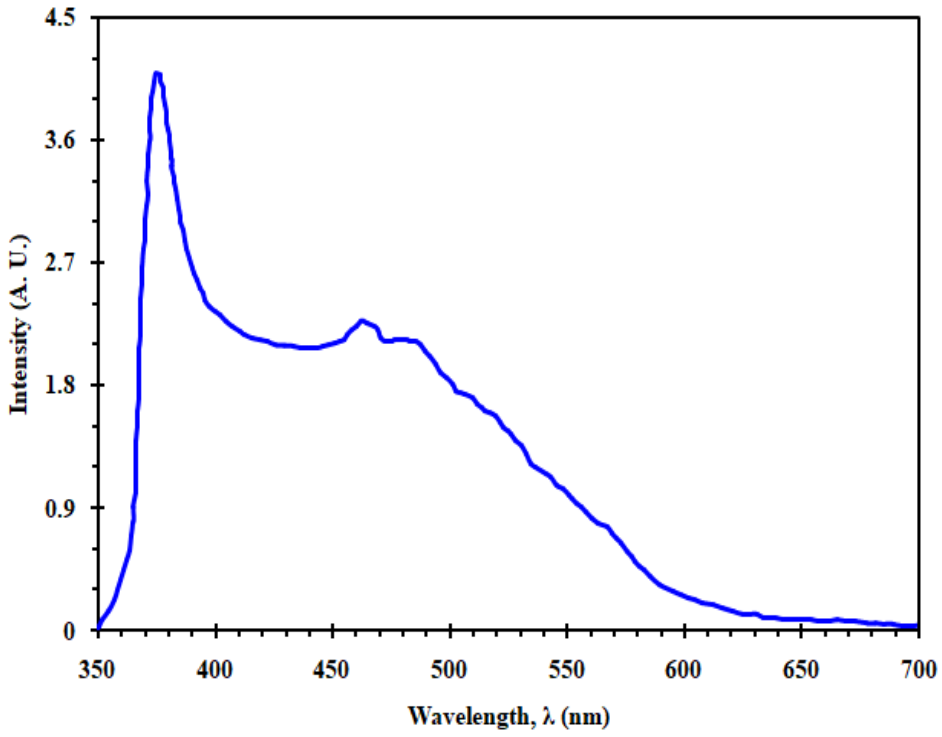


**Fig.9:** PL spectra of sol-gel synthesis of ZnO NPs.

## IV. Conclusions

ZnO nanoparticles were successfully synthesized*via* a simple sol-gel technique. Based on XRD data, all of the diffraction peaks of ZnO NPs were indexed to(100), (002), (101), (102), (110), (103), (200), (112), (201), (004) and (202) reflections corresponding to the pure hexagonal wurtzite structure of ZnO with lattice constant values $a = b = 3.2488$ Å and $c = 5.2054$ Å. The average crystal size calculated by the Debye Scherrer's equation was found to be 28 nm.The average particle size estimated from ESEM micrographs for sol-gel synthesis of ZnONPs was nearly 60 nm. The EDS study confirmed the presence of Oxygen and Zinc in the synthesized nanoparticles.FTIR spectroscopy suggested that ZnONPs exhibited a broad band at the wavenumber of 3507 $cm^{-1}$and this band shows the presence of O-H stretching vibration which is due to absorbed moisture on the surface of the samples.Theabsorption picks around 1392 $cm^{-1}$ is assigned to thebending vibration of C-H stretching. The peaks at 514 to442 $cm^{-1}$ are for Zn-O. The obtained value of the optical band gap using UV-Vis reflectance was 3.18 eV. The PL spectra of the sol-gel synthesis of the ZnONPs presented a strong emission band located at the wavelength of 375 nmwhich is typical UV band. This may be ascribed to the exciton recombination related near-band edge emission ofZnO. A week blueband at 465 nm was also observed which is due to the electron transition from the conduction band to interstitialoxygen defects ($O_{in}$) in the ZnO.

## Acknowledgments

The financial support of University Grant Commission, Bangladesh,to carry out this project is gratefully acknowledged by Authors.

## References:

[1]. S.T. Khan, J. Musarrat, A.A. Al-Khedhairy, Countering drug resistance, infectious diseases, and sepsis using metal and metal oxides nanoparticles: Current status, Colloids and Surfaces B: Biointerfaces 146 (2016) 70-83.
[2]. S.K. Das, J.M. Islam, M. Hasan, H. Kabir, M.A. Gafur, E. Hoque, M.A. Khan, Astronomy, Development of electrically conductive nanocrystalline thin film for optoelectronic applications, J International Letters of Chemistry, Physics 10 (2013) 90-101.
[3]. M. Sastry, A. Ahmad, M.I. Khan, R. Kumar, Biosynthesis of metal nanoparticles using fungi and actinomycete, J Current science 85(2) (2003) 162-170.
[4]. A. Amri, K. Hasan, H. Taha, M.M. Rahman, S. Herman, Andrizal, E. Awaltanova, I. Wantono, H. Kabir, C.-Y. Yin, K. Ibrahim, S. Bahri, N. Frimayanti, M.A. Hossain, Z.-T. Jiang, Surface structural features and optical analysis of nanostructured Cu-oxide thin film coatings coated via the sol-gel dip coating method, Ceramics International 45(10) (2019) 12888-12894.
[5]. M.D. Rao, P. Gautam, Synthesis and characterization of ZnO nanoflowers using Chlamydomonas reinhardtii: A green approach, Environmental Progress & Sustainable Energy 35(4) (2016) 1020-1026.
[6]. M. Mia, U. Habiba, M. Pervez, H. Kabir, S. Nur, M. Hossen, S. Sen, M.K. Hossain, M.A. Iftekhar, M.M. Rahman, Investigation of aluminum doping on structural and optical characteristics of sol–gel assisted spin-coated nano-structured zinc oxide thin films, J Applied Physics A 126(3) (2020) 162.
[7]. M.S. Hossain, H. Kabir, M.M. Rahman, K. Hasan, M.S. Bashar, M. Rahman, M.A. Gafur, S. Islam, A. Amri, Z.-T. Jiang, M. Altarawneh, B.Z. Dlugogorski, Understanding the shrinkage of optical absorption edges of nanostructured Cd-Zn sulphide films for photothermal applications, Applied Surface Science 392 (2017) 854-862.
[8]. F. Charbgoo, M.B. Ahmad, M. Darroudi, Cerium oxide nanoparticles: green synthesis and biological applications, International journal of nanomedicine. 12 (2017) 1401-1413.
[9]. P.C. Nagajyothi, P. Muthuraman, T.V.M. Sreekanth, D.H. Kim, J. Shim, Green synthesis: In-vitro anticancer activity of copper oxide nanoparticles against human cervical carcinoma cells, Arabian Journal of Chemistry 10(2) (2017) 215-225.
[10]. W.-N. Wang, I.W. Lenggoro, Y. Terashi, T.O. Kim, K. Okuyama, One-step synthesis of titanium oxide nanoparticles by spray pyrolysis of organic precursors, Materials science & engineering. 123(3) (2005) 194-202.
[11]. H. Kabir, S.H. Nandyala, M.M. Rahman, M.A. Kabir, A. Stamboulis, Influence of calcination on the sol–gel synthesis of lanthanum oxide nanoparticles, Applied physics. 124(12) (2018) 820.
[12]. H. Kabir, S.H. Nandyala, M.M. Rahman, M.A. Kabir, Z. Pikramenou, M. Laver, A. Stamboulis, Polyethylene glycol assisted facile sol-gel synthesis of lanthanum oxide nanoparticles: Structural characterizations and photoluminescence studies, Ceramics International 45(1) (2019) 424-431.
[13]. H. Mirzaei, M. Darroudi, Zinc oxide nanoparticles: Biological synthesis and biomedical applications, Ceramics International 43(1) (2017) 907-914.
[14]. V. Patel, D. Berthold, P. Puranik, M. Gantar, Screening of cyanobacteria and microalgae for their ability to synthesize silver nanoparticles with antibacterial activity, Biotechnology Reports 5(1) (2015) 112-119.
[15]. M. Stan, A. Popa, D. Toloman, A. Dehelean, I. Lung, G. Katona, Enhanced photocatalytic degradation properties of zinc oxide nanoparticles synthesized by using plant extracts, Materials Science in Semiconductor Processing 39 (2015) 23-29.
[16]. E.D. Sherly, J.J. Vijaya, N.C.S. Selvam, L.J. Kennedy, Microwave assisted combustion synthesis of coupled ZnO–ZrO2 nanoparticles and their role in the photocatalytic degradation of 2,4-dichlorophenol, Ceramics International 40(4) (2014) 5681-5691.
[17]. G. Sangeetha, S. Rajeshwari, R. Venckatesh, Green synthesis of zinc oxide nanoparticles by aloe barbadensis miller leaf extract: Structure and optical properties, Materials Research Bulletin 46(12) (2011) 2560-2566.
[18]. K. Elumalai, S. Velmurugan, Green synthesis, characterization and antimicrobial activities of zinc oxide nanoparticles from the leaf extract of Azadirachta indica (L.), Applied Surface Science 345 (2015) 329-336.
[19]. Z. Sheikhloo, M. Salouti, F. Katiraee, Biological Synthesis of Gold Nanoparticles by Fungus Epicoccum nigrum, Including Nanoclusters and Nanoparticles 22(4) (2011) 661-665.
[20]. K. Chitra, G. Annadurai, Antimicrobial activity of wet chemically engineered spherical shaped ZnO nanoparticles on food borne pathogen, International Food Research Journal 20(1) (2013) 59-64.
[21]. R. Ikono, P.R. Akwalia, W.B.W. Siswanto, A. Sukarto, N.T. Rochman, Effect of PH variation on particle size and purity of nano zinc oxide synthesized by sol-gel method, J Int. J. Engl. Technol 12 (2012) 5-9.

[22]. H. He, Q. Yang, J. Wang, Z. Ye, Layer-structured ZnO nanowire arrays with dominant surface- and acceptor-related emissions, Materials Letters 65(9) (2011) 1351-1354.
[23]. J. Sawai, Quantitative evaluation of antibacterial activities of metallic oxide powders (ZnO, MgO and CaO) by conductimetric assay, Journal of Microbiological Methods 54(2) (2003) 177-182.
[24]. X.H. Huang, R.Q. Guo, J.B. Wu, P. Zhang, Mesoporous ZnO nanosheets for lithium ion batteries, Materials Letters 122 (2014) 82-85.
[25]. L.-H. Li, J.-C. Deng, H.-R. Deng, Z.-L. Liu, L. Xin, Synthesis and characterization of chitosan/ZnO nanoparticle composite membranes, Carbohydrate Research 345(8) (2010) 994-998.
[26]. [26] Y. Yang, X. Li, J. Chen, H. Chen, X. Bao, ZnO nanoparticles prepared by thermal decomposition of β-cyclodextrin coated zinc acetate, Chemical Physics Letters 373(1-2) (2003) 22-27.
[27]. J.J. Wu, S.C. Liu, Low-Temperature Growth of Well-Aligned ZnO Nanorods by Chemical Vapor Deposition, Advanced Materials 14(3) (2002) 215-218.
[28]. P. Tonto, O. Mekasuwandumrong, S. Phatanasri, V. Pavarajarn, P. Praserthdam, Preparation of ZnO nanorod by solvothermal reaction of zinc acetate in various alcohols, J Ceramics International 34(1) (2008) 57-62.
[29]. M. Vafaee, M.S. Ghamsari, Preparation and characterization of ZnO nanoparticles by a novel sol–gel route, Materials Letters 61(14) (2007) 3265-3268.
[30]. S. Nagarajan, K. Arumugam Kuppusamy, Extracellular synthesis of zinc oxide nanoparticle using seaweeds of gulf of Mannar, India, Journal of Nanobiotechnology 11(1) (2013) 39.
[31]. A. Bari, M. Shinde, V. Deo, L. Patil, Effect of solvents on the particle morphology of nanostructured ZnO, Indian Journal of Pure and Applied Physics 47(1) (2009) 24-27.
[32]. M. Przybyszewska, M. Zaborski, Effect of ionic liquids and surfactants on zinc oxide nanoparticle activity in crosslinking of acrylonitrile butadiene elastomer, J Journal of applied polymer science 116(1) (2010) 155-164.
[33]. Y. Wang, X. Li, N. Wang, X. Quan, Y. Chen, Controllable synthesis of ZnO nanoflowers and their morphology-dependent photocatalytic activities, Separation and Purification Technology 62(3) (2008) 727-732.
[34]. R.J. Cernik, X-ray Powder Diffractometry. An Introduction. (Serie: Chemical Analysis, Vol. 138.) VonR. Jenkins undR. L. Snyder. John Wiley & Sons, New York, 1996. 391 S., geb. 87.95 £.—ISBN 0–471–51339–3, Angewandte Chemie 109(12) (1997) 1417-1418.
[35]. R. John, R. Rajakumari, Synthesis and Characterization of Rare Earth Ion Doped Nano ZnO, Nano-Micro Letters 4(2) (2012) 65-72.
[36]. F. Ozutok, B. Demirselcuk, E. Sarica, S. Turkyilmaz, V. Bilgin, Study of Ultrasonically Sprayed ZnO Films: Thermal Annealing Effect, Acta Physica Polonica A 121(1) (2012) 53-55.
[37]. E. Goharshadi, T. Mahvelati, M. Yazdanbakhsh, Influence of preparation methods of microwave, sol–gel, and hydrothermal on structural and optical properties of lanthania nanoparticles, Journal of the Iranian Chemical Society 13(1) (2016) 65-72.
[38]. A.K. Zak, R. Razali, W.H.A. Majid, M. Darroudi, Synthesis and characterization of a narrow size distribution of zinc oxide nanoparticles, International journal of nanomedicine 6 (2011) 1399-1403.
[39]. P.K.F.J. Munk, J. Tech. Phys. 12 (1931) 593-601.
[40]. I. Alibe, K. Matori, E. Saion, A. Ali, M. Zaid, The Influence of Calcination Temperature on Structural and Optical Properties of ZnO Nanoparticles via Simple Polymer Synthesis Route, Science of Sintering 49(3) (2017) 263-275.
[41]. A. Bedia, F.Z. Bedia, M. Aillerie, N. Maloufi, S. Ould Saad Hamady, O. Perroud, B. Benyoucef, Optical, electrical and structural properties of nano-pyramidal ZnO films grown on glass substrate by spray pyrolysis technique, Optical Materials 36(7) (2014) 1123-1130.
[42]. F.Z. Haque, N. Singh, P. Pandey, M.R. Parra, Study of Zinc Oxide nano/micro rods grown on ITO and glass substrates, Optik - International Journal for Light and Electron Optics 124(20) (2013) 4167-4171.
[43]. M. Ramzan Parra, F.Z. Haque, Structural and optical properties of poly-vinylpyrrolidone modified ZnO nanorods synthesized through simple hydrothermal process, Optik - International Journal for Light and Electron Optics 125(17) (2014) 4629-4632.


Umme Habiba, etal. "Synthesis of Zinc Oxide Nanoparticles via Sol-gel Technique." *IOSR Journal of Applied Physics (IOSR-JAP)*, 12(2), 2020, pp. 10-19.